Biophysical Journal, Volume 96

Supporting Material

Self-Assembly of Phenylalanine Oligopeptides: Insights from Experiments and Simulations

Phanourios Tamamis, Lihi Adler-Abramovich, Meital Reches, Karen Marshall, Pawel Sikorski, Louise Serpell, Ehud Gazit, and Georgios Archontis

Self-Assembly of Phenylalanine Oligopeptides: Insights from Experiments and Simulations

Phanourios Tamamis, Lihi Adler-Abramovich, Meital Reches, Karen Marshall, Pawel Sikorski, Louise Serpell, Ehud Gazit and Georgios Archontis

Supplementary Material

Methods

I. Experimental Methods.

Preparation of Initial Solutions of Peptides – Peptides were purchased from Bachem (Bubendorf, Switzerland). Fresh stock solutions were prepared by dissolving lyophilized form of the peptides in 1,1,1,3,3,3-hexafluoro-2-propanol (HFP), purchased from Sigma-Aldrich, at a concentration of 100 mg/ml. To avoid any pre-aggregation, fresh stock solutions were prepared for each experiment. Peptide stock solution was diluted in double distilled (dd) H_2O to a final concentration of 2 mg/ml.

Transmission Electron Microscopy – A 10μl aliquot of the peptides solution was placed on 400 mesh copper grid. After 1 minute, excess fluid was removed. For negative staining, the grid was stained with 2% uranyl acetate in water and after two minutes excess fluid was removed from the grid. Samples were viewed using a JEOL 1200EX electron microscope operating at 80 kV.

Scanning Electron Microscopy – A 10 μl aliquot of the solution was dried at room temperature on a microscope glass cover slip and coated with gold. Scanning electron microscopy images were made using a JSM JEOL 6300 SEM operating at 5 kV.

Environmental Scanning Electron Microscopy – A 5 μl aliquot of the solution was placed on a metal stand. Environmental scanning electron Microscopy images were made using Quanta 200 FEG Field Emission Gun ESEM operating at 10 kV.

ThT Staining and Confocal Laser Microscopy Imaging – 10 μl ThT solution (2 mM, PBS buffer) were mixed with 10 μl peptide solutions. An LSM 510 confocal laser scanning microscope (Carl Zeiss Jena, Germany) was used at excitation and emission wavelengths of 440 and 485 nm, respectively.

Fourier Transform Infrared Spectroscopy – Infrared spectra were recorded using Nicolet Nexus 470 FT-IR spectrometer with DTGS detector. Peptide solutions samples were dried by vacuum on CaF_2 plate to form thin film. The peptide deposits was resuspended with D_2O and dried. The resuspension procedure was repeated twice to ensure maximal hydrogen to deuterium exchange. The measurements were taken using a 4 cm^{-1} resolution and 2000 scans averaging. The transmittance minima values were determined by OMNIC analysis program (Nicolet).

II. Computational methods.

Force Field – The peptide atomic charges, *van der Waals* and stereochemical parameters were taken from the CHARMM22 all-atom force field (ref. 47 in main text). The FF and FFF molecules had charged N-terminal (NH_3^+) and C-terminal (COO^-) ends, as in the experiments. Solvent effects were taken into account by the GBSW implicit-solvent model, with the optimized parameters and backbone torsional (CMAP) correction (refs. 45 and 46 in main text). The nonpolar solvation energy was proportional to the solvent-exposed surface area, with the surface-tension proportionality coefficient set to 0.005 kcal/mol/$Å^2$ (ref. 46 in main text). The non-bonded interactions between atom-pairs were switched to zero for distances larger than 22 Å. The lengths of covalent bonds involving hydrogen atoms were constrained to standard values by the SHAKE algorithm (1)[a].

Simulation Methodology – Each solution was simulated by the replica-exchange method. We conducted preliminary replica simulations in the temperature range 288 K – 412 K. The average potential energies and acceptance exchange probabilities obtained from these simulations were used in the iterative optimization of the replica temperatures as in (refs. 43, 44 in main text), targeting a uniform exchange probability ~18-20% between adjacent (in temperature) replicas. In the final setup, the peptides were initially placed at random positions and orientations in the simulation box, with conformations taken from separate simulations of the FF and FFF monomers; the FF and FFF solutions employed 10 replicas, spanning the temperature ranges 289-405 K and 288-416 K,

[a] For references not included in main text, a separate list is at the end of SM.

respectively. The employed temperatures and the achieved acceptance probabilities are listed in table S1. In both systems, all replicas executed random walks in the entire temperature range.

The equations of motion were solved with the leap-frog algorithm, using a 2-fs time step. The temperature was controlled by the Langevin method; the Langevin friction coefficients were set to 5.0 ps^{-1} for heavy atoms.

The total simulation length was 40 ns at each temperature (0.4 μs for the 10 replicas). Exchanges between adjacent replicas were attempted at 10-ps intervals. The analysis was performed with the CHARMM modules, the VMD (ref. 52 in main text) and Vega (2) packages, and in-house programs. Analysis of the average structural properties of the systems showed that the replica simulations reached equilibrium rapidly (within the first few ns). As an example, in fig. S1 we plot the average number of peptide networks, observed in the simulations, as a function of simulation time. The averages reported in the paper employed 20,000 snapshots at 2-ps intervals, spanning the 40-ns replica simulations.

Computation of peptide network association energies –The association energy of a network with X peptides was computed by the expression

$$\Delta E_{\text{assoc}}(X) = E_{\text{network}}(X) - \sum_{i=1}^{X} E_i \qquad (1)$$

The network energy, $E_{\text{network}}(X)$, included the intra- and intermolecular energies among the constituent peptides. The effect of surrounding environment (other peptides and solvent) was included in the GB energies via the atomic solvation radii, and in the nonpolar solvation free-energies via the solvent-accessible surface area. The monomer energies E_i were computed by assuming that each of the network peptides i had the same conformation as in the network, but was isolated and immersed in solution. Thus, all

intramolecular contributions to the association energy $\Delta E_{\text{assoc}}(X)$ cancelled, except for the GB and non-polar solvation energies.

Definition of linear networks. A peptide network consists of n peptides, hydrogen-bonded via consecutive head-to-tail interactions (scheme I).

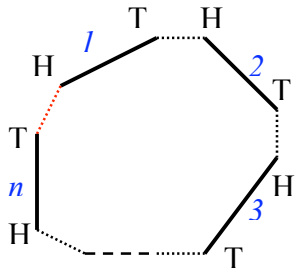

Scheme I: An n-member peptide network. Head and tail atoms are marked as "H" and "T". The dotted lines denote head-to-tail interactions. If the red dotted line does not exist, the network is open.

(1) A network of two peptides (n=2) is closed (R2), if it has two H-T interactions. For n>2, the network is closed (Rn) if there is a head-to-tail interaction between the first and the n-th peptide. (In this case, any peptide in the network can be designated as "first"). Otherwise, the network is open (On).

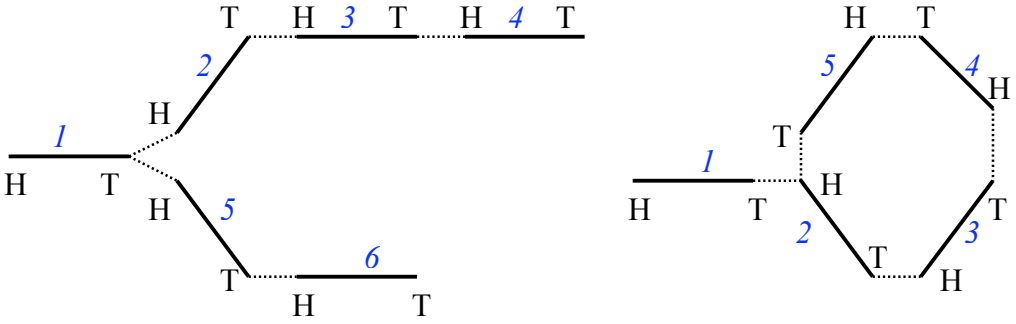

Scheme II: Examples of branched networks.

(2) If the head (tail) of a peptide hydrogen-bonds to at least two tails (heads) of two other peptides, the network is branched. We do not count these networks separately, but

consider them as combinations of linear and closed networks. The left panel of scheme II shows a branched network, which we count as two linear networks O4 (peptides 1, 2, 3, 4) and O3 (peptides 1, 5, 6). The right panel of scheme 2 shows a closed branched network, which we count as one closed network R4 (peptides 2, 3, 4, 5) and one open network O2 (peptides 1, 2).

Our FORTRAN source code for the network determination is available upon request.

Temperatures employed in the replica simulations.

Table S1. Temperatures (in K) employed in the FF and FFF replica simulations. The acceptance probabilities for exchanges of adjacent replicas (in temperature) are enclosed in parentheses.

Solution	Replica temperatures (exchange probabilities)
FF	289 (0.18) 300 (0.17) 312 (0.18) 324 (0.22) 336 (0.18) 349 (0.21) 363 (0.19) 376 (0.21) 390 (0.19) 405
FFF	288 (0.19) 300 (0.20) 312 (0.16) 326 (0.20) 339 (0.18) 353 (0.20) 368 (0.20) 383 (0.20) 399 (0.20) 416

Convergence of the REMD simulations. Fig. S1 plots the average number of networks/snapshot for the 300 K simulations, as a function of the simulation time. In both systems, the various averages converge in the first 5-10 ns. If we treat the first 5 ns as equilibration and use only the 5 – 40 ns period to compute the averages reported in table 1 of the main text, the results remain essentially identical (not shown).

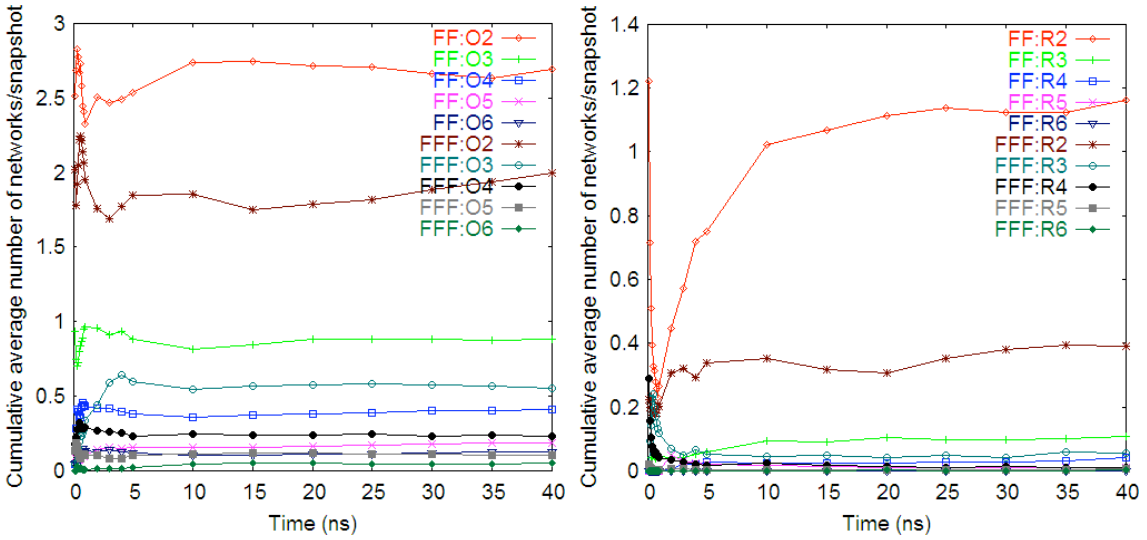

Fig. S1. The cumulative average number of networks/snapshot for the 300 K simulations is plotted against the time. Left and right panels correspond to open and closed-ring like networks, respectively.

Results

Typical peptide networks, observed in the simulations. Fig. S2 shows representative closed (ring-like) network conformations of five or four peptides, observed in the room-temperature FF and FFF simulations.

Frequency dependence of the FF and FFF networks on the simulation temperature. The average numbers of peptide networks observed per snapshot are plotted as a function of temperature and network size (number of peptides) in fig. S3. Open and ring-like networks are considered together; the ring contribution to the total number is always less than 10%. The FF probabilities have been scaled by an appropriate combinatorial factor (footnote of table 1, main text), which accounts for the larger monomer number in the FF system. The network propensity decreases with temperature in both FF and FFF aggregates, as expected; the higher relative propensity of FFF with respect to FF is maintained at all temperatures.

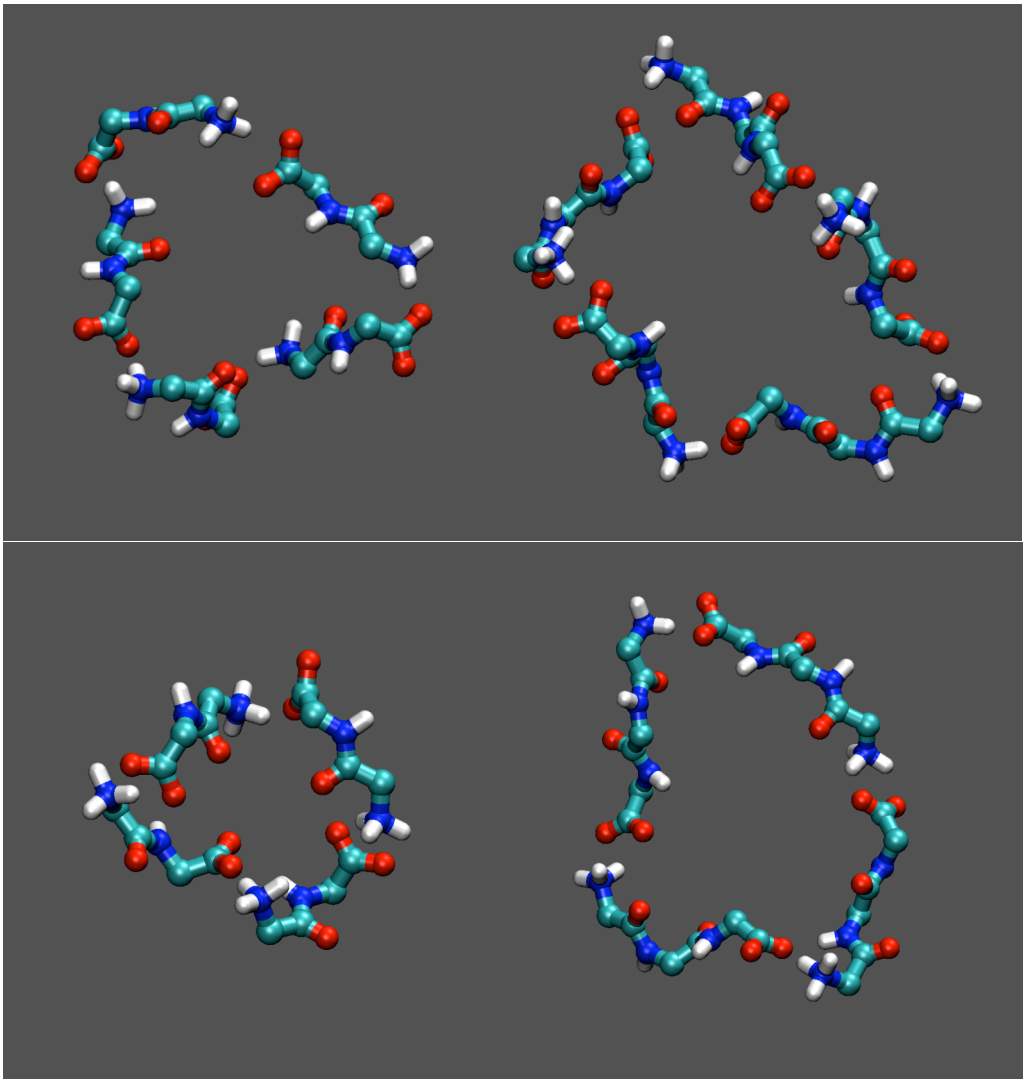

Fig. S2. Representative ring-like networks of five (top) and four (bottom) peptides, observed in the FF (left) and FFF (right) simulations at 300 K. Only the main chain atoms of the network are shown in licorice/CPK representation; other network atoms and the surrounding aggregate are omitted.

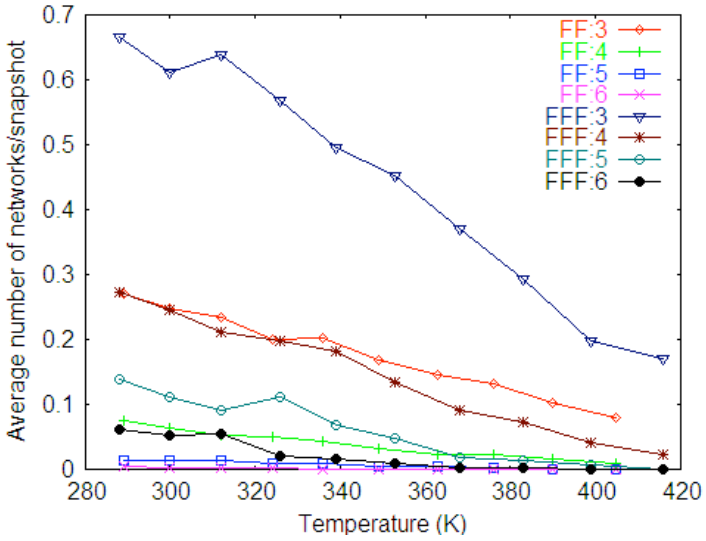

Fig. S3. Temperature dependence of the average number of networks/snapshot, observed in the FF and FFF simulations. Open and closed (ring-like) networks are considered together (in each case, the ring-network contribution is less than 10% of the total). The FF probabilities have been scaled by an appropriate factor (see footnote of table 1, main text), which accounts for the larger monomer number in the FF system (12), compared to FFF (8).

Examples of planar, periodic conformations with antiparallel beta-sheet interactions. Here, we show some examples of planar conformations, periodic in two-dimensions, which contain some of the hydrogen-bonding patterns observed in the FF sheets of the simulations (table 3 and fig. 5 in main text).

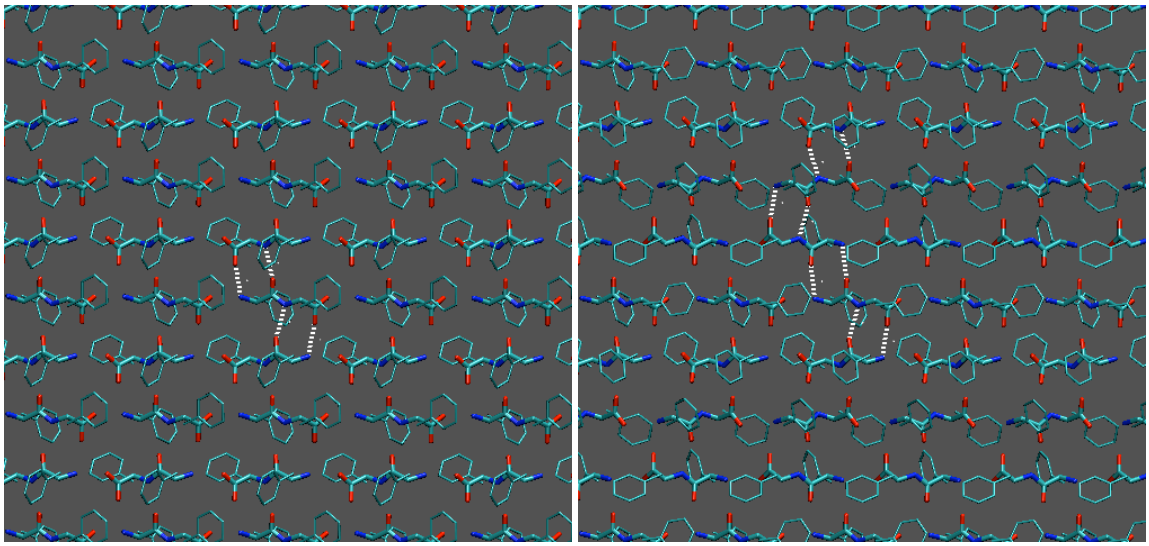

Fig. S4. Left: Planar FF structure, with aligned antiparallel strands. The hydrogen-bonding patterns are as in the second FF family of table 3 (fig. 5d) of the main text. **Right:** Planar FF structure with partly aligned/partly unaligned antiparallel strands. The indicated hydrogen-bonding patterns correspond (from top to bottom) to families 1, 2, 4 and 2. Head/tail interactions along each strand are omitted for clarity.

To create these conformations, we set the backbone dihedral angles of the FF monomer to the ideal antiparallel β-sheet values phi=-139^{o}, psi=+135^{o} and the other internal coordinates to the default parameters of the CHARMM force field. We then translated the monomer via the program *gOpenMol* (3), to create periodic conformations of 6x12 peptides. In both cases, we adjusted the side-chain dihedral angles in order to avoid steric conflicts among strands. The inter- and intra-strand distances were optimized with CHARMM and the same GBSW force field used in the simulations. In the final aligned and unaligned conformations, the distance between strands is 4.7 Å.

Energy calculations with these finite sheets showed that the aligned conformation (left plot) is favored with respect to the partly unaligned/partly aligned conformation (right plot), mainly due to polar interactions (2.7 kcal/mol/peptide). The unaligned strands contain only the two internal hydrogen-bonding patterns (out of four) of the high-frequency family 1 (fig. 5a) and the patterns of low-frequency family 3 (fig. 5c). Both conditions were necessary to create this periodic structure, and may contribute to its lower stability, compared to the aligned conformation.

Orientation of Side-Chains within the FF and FFF monomers. The relative placement of the two FF side-chains with respect to the intermediate peptide bond can be described by the pseudodihedral angle $\theta \equiv C_{\beta 1}$- $C_{\alpha 1}$- $C_{\alpha 2}$- $C_{\beta 2}$. The probability density of θ at 300 ^{o}K is small near 180^{o}, and has two maxima near -70^{o} and 25^{o} (Fig. S5). Thus, the two side-chains mostly point toward the same side of the peptide bond, as in the FF crystals (where $\theta \approx 40^{o}$). In the FFF molecule, the relative orientations of side-chains 1 and 2 (2 and 3) are described by $\theta_1 \equiv C_{\beta 1}$- $C_{\alpha 1}$- $C_{\alpha 2}$- $C_{\beta 2}$ ($\theta_2 \equiv C_{\beta 2}$- $C_{\alpha 2}$- $C_{\alpha 3}$- $C_{\beta 3}$). Angle θ_1 has peaks near -70^{o} and 30^{o} and θ_2 has peaks near 35^{o} and -130^{o} (Fig. S5). Thus, in the case of FF the first two side-chains of a monomer were usually placed at the same side of the intermediate peptide bond (as in FF), but the third side-chain could point at the opposite direction.

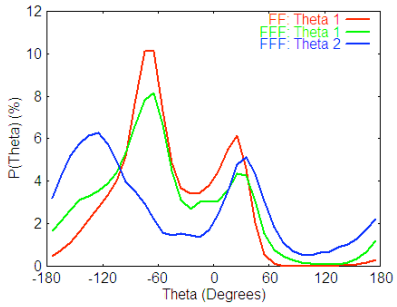

Fig. S5. Probability distribution of the pseudodihedral angles θ (FF) and θ_1, θ_2 (FFF) in the simulations at 300 K.

Relative orientation of the phenylalanine rings, in intra- and intermolecular pairs of adjacent (in space) sidechains. The contact geometry of nearest-neighbor phenylalanine side-chain planes can be described by the distance (r) between the aromatic ring centers, the angle (χ) between the aromatic rings and the two angles (φ_1, φ_2) between the vector connecting the two ring centers and the normals to the aromatic ring planes (Scheme III).

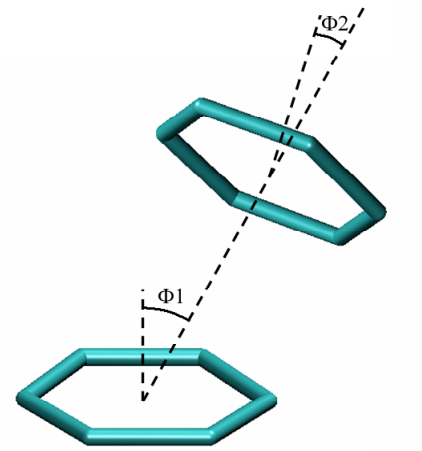

Scheme III. Definition of the angles φ_1 and φ_2 employed to characterize the relative orientation of interacting aromatic side-chains.

In the FF crystals [refs. 36, 37 in main text], intermolecular pairs of nearest-neighbor side-chains adopt contact distances r~6.5 Å along the same hexagonal ring, or r=5.3–6 Å on adjacent channels and T-shaped orientations (χ=90°); for intramolecular pairs, the corresponding values are r=5.6 Å and χ =58°.

The two-dimensional (2D) probability densities $P(\varphi_1, \varphi_2)$ at 300 K, for pairs of nearest-neighbor aromatic rings (r < 7 Å) and various ranges of χ values are shown in Fig. S6. The first and last two rows correspond, respectively, to inter- and intramolecular pairs.

A large fraction of conformations (47%) adopt approximately T-shaped orientations (angles χ=60°-90°), as in the crystals. Fig. S7 shows a representative six-member ring from the 300 K FF simulations, containing several T-shaped side-chain interactions. Conformations with somewhat smaller angles (χ=30°-60°) are also probable (37%), but parallel-displaced orientations (χ=0°-30°) are less frequent (16%). The FF crystals (refs. 36, 37 in main text) do contain parallel-displaced nearest-neighbor side chains, which belong to peptides on adjacent rings, along the same channel. The backbones of these peptides are parallel and form head-head and tail-tail contacts; the parallel backbone orientations are nevertheless stabilized via multiple interactions with opposite-charge

termini of surrounding peptides. In the simulations, the parallel orientation of two peptides is rarely encountered (main text, table 2); this may explain the reduced probability of the aromatic displaced-parallel orientations.

The intramolecular nearest-neighbor pairs (last two rows of Fig. S6) adopt also conformations with χ=30°-90°. The inter- and intramolecular probabilities P(φ_1, φ_2) are somewhat narrower in the FFF system, presumably due to the increased FFF molecular size. Nevertheless, it is noteworthy that the fractions of conformations in the various χ ranges are very similar in the FF and FFF system.

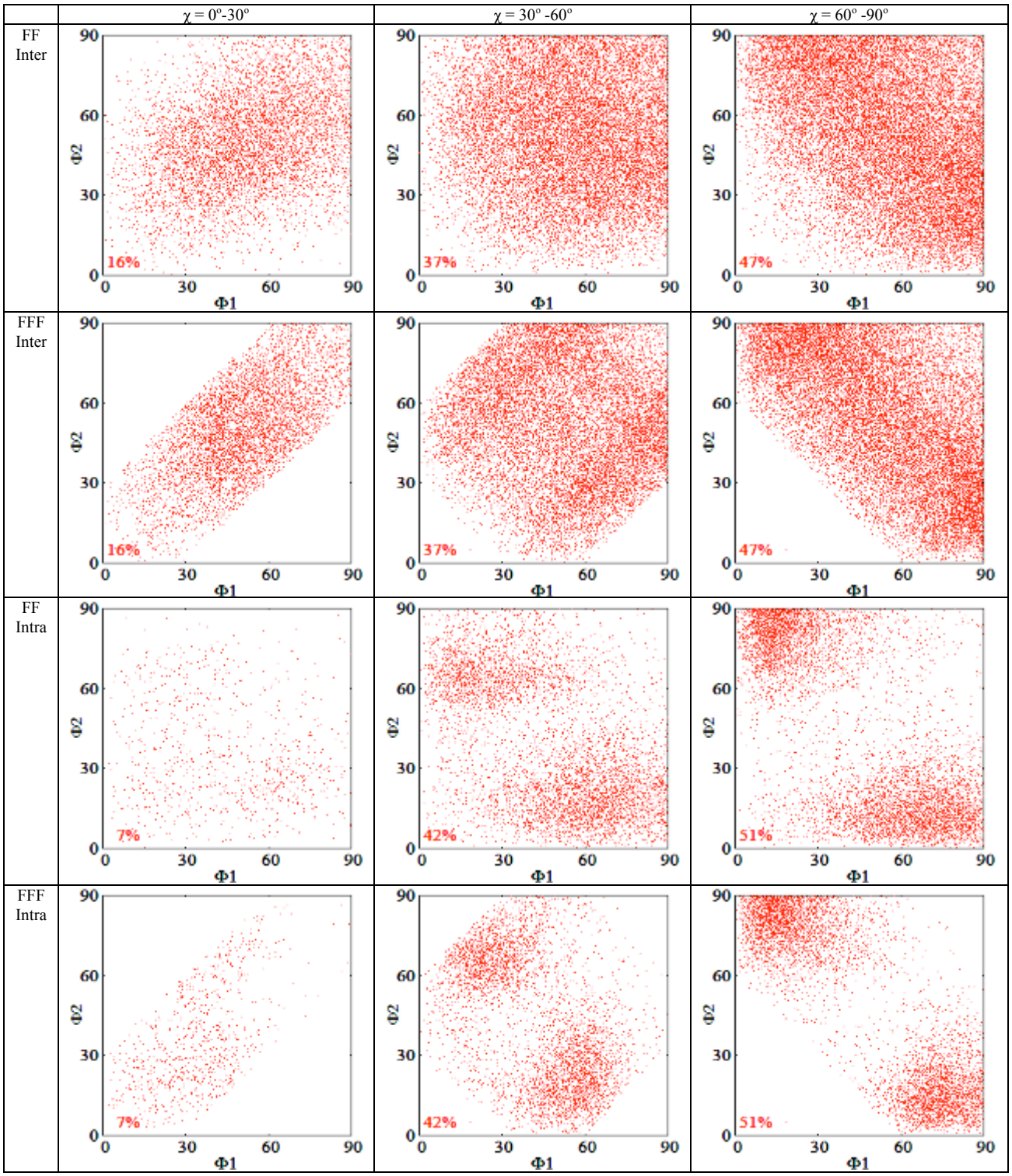

Fig. S6. 2D probability densities $P(\varphi_1, \varphi_2)$ (at 300 K), for pairs of interacting aromatic rings (the distances between ring centers in each pair are less than 7 Å). The first and last two rows correspond, respectively, to inter- and intramolecular side chain pairs. The panels (left to right) correspond to the ranges χ=0°-30°, 30° -60°, 60° -90°. The fraction of conformations in each χ range is included in the plots.

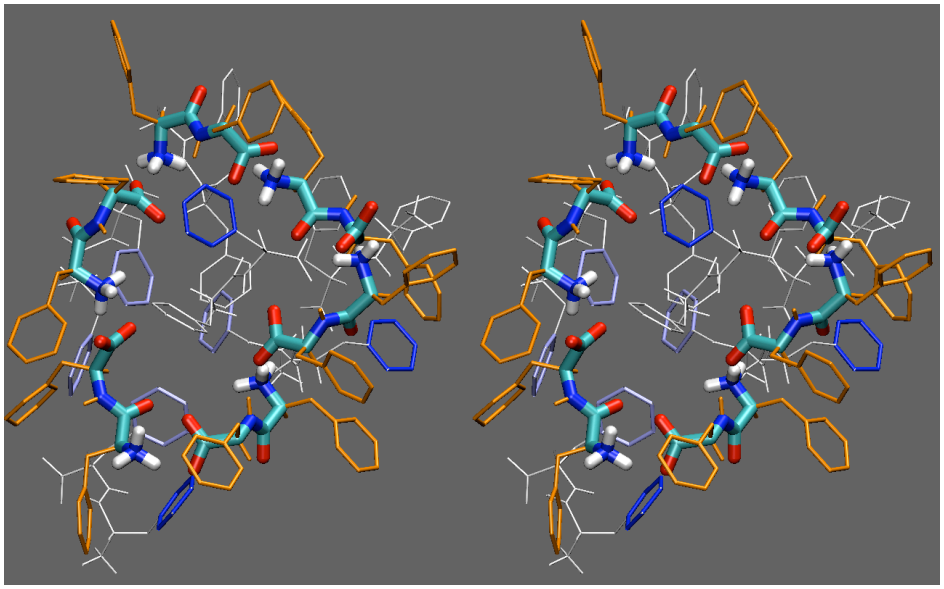

Fig. S7. Stereo representation of a characteristic six-member ring conformation from the FF simulations at 300 K. The peptide backbones and side-chains are shown in thick licorice, colored, respectively, by atom-type or orange coloring. The remaining, surrounding aggregate is shown in white, except for side-chains interacting with the ring (in blue) or with each other (in ice blue).

Supplementary Material References

1. Ryckaert, J. P., G. Ciccotti and H. J. C. Berendsen. 1977. Numerical integration of the cartesian equations of motion of a system with constraints: molecular dynamics of n alkanes. J. Comput. Phys. 23:327–341.

2. Pedretti, A., L. Villa and G. Vistoli. 2002. VEGA: A versatile program to convert, handle and visualize molecular structure on windows-based PCs. J. Mol. Graph. 21:47-49.

3. Laaksonen, L. 1992. A graphics program for the analysis and display of molecular dynamics trajectories. J. Mol. Graph. 10:33-34.